Journal of Physics D: Applied Physics

Radiation tolerance of GaN: the balance between radiation-stimulated defect annealing and defect stabilization by implanted atoms

Radiation tolerance of GaN: the balance between radiation-stimulated defect annealing and defect stabilization by implanted atoms

A. I. Titov[1], K. V. Karabeshkin[1], A. I. Struchkov[1], P. A. Karaseov[1], and A. Azarov[2]

[1] *Peter the Great St.-Petersburg Polytechnic University, St.-Petersburg, Russia*

[2] *Centre for Materials Science and Nanotechnology, University of Oslo, Oslo, Norway*

Realization of radiation-hard electronic devices able to work in harsh environments requires deep understanding the processes of defect formation/evolution occurring in semiconductors bombarded by energetic particles. In the present work we address such intriguing radiation phenomenon as high radiation tolerance of GaN and analyze structural disorder employing advanced co-irradiation schemes where low and high energy implants with different ions have been used. Channeling analysis revealed that the interplay between radiation-stimulated defect annealing and defect stabilization by implanted atoms dominates defect formation in the crystal bulk. Furthermore, the balance between these two processes depends on implanted species. In particular, strong damage enhancement leading to the complete GaN bulk amorphization observed for the samples pre-implanted with fluorine ions, whereas the co-irradiation of the samples pre-implanted with such elements as neon, phosphorus, and argon ions leads to a decrease of the damage.

1. Introduction

Understanding radiation tolerance of materials is crucial for applications in harsh environments where electronic devices can undergo a long time exposure by different energetic particles [1]. Despite that radiation defect formation in electronic and nuclear materials has been extensively investigated during the last several decades [2, 3] many radiation phenomena are still not fully studied and understood. For example, the origin of high radiation resistance of semiconductors having a high degree of ionicity of chemical bonds remains unclear. In particular, it holds to gallium nitride (GaN), which is a wide bandgap (3.4 eV) semiconductor having number of applications for high power, microwave and optoelectronic devices [4-6]. It was shown that the damage buildup in GaN under ion bombardment exhibits intriguing behavior different from that for other semiconductors. In particular, it was established that radiation damage depth distribution in GaN consists of two major peaks demonstrating different behavior with increasing ion dose [7-9]. The first one corresponds to an amorphous/nanocrystalline layer formed at the surface [8, 10-12] and this peak is hereinafter referred to as surface amorphous layer (SAL). The second damage peak is situated in the crystal bulk and we refer to it as the bulk defect peak (BDP). This peak originates at the depth close to the maximum of elastic energy deposition of stopping ions. With the ion dose increase, SAL becomes broader, while BDP grows up with an apparent shift of its depth position deeper into the bulk of the material. Disorder in the BDP consists of interstitial-based planar defects parallel to the (0001) planes [8, 10, 12-15] in addition to point defect clusters and it exhibits saturation at ~40–50% of full amorphization level for room temperature implants [3, 8, 9, 13-16]. In its turn, the interface between SAL and the bulk crystalline material (a/c interface) acts as a nucleation site for the amorphization of the target, which proceeds from the surface to the crystal bulk [8, 17, 18].

High radiation resistance of different semiconductors was previously attributed to the enhanced defect annihilation at extended defects [19, 20], strong ion-induced recrystallization effects [21] or pronounced role of the a/c interface which acts as a perfect sink for mobile point defects (MPDs) generated by stopping ions in the crystal bulk [17]. Note that the latter model explains not only the damage saturation in GaN bulk but also a shift of the bulk disorder maximum position with increasing ion dose. An additional argument in favor of this model is a non-commutative damage accumulation in GaN that was experimentally observed recently for F ions [22]. However, various chemical effects of implanted ions can play a role in damage formation in GaN which were not taken into account in the models proposed. For example, it was demonstrated that implanted carbon atoms can form triple -C≡N- nitrilelike carbon-nitride bonds and suppress ion-beam-induced material decomposition [23]. Moreover, C atoms enhance disorder buildup and facilitate amorphization of GaN [8, 24]. Damage formed by fluorine and neon ions is the same at the initial stage [25], but some chemical effect of F is manifested in ion-beam-induced surface topography change [26]. Fluorine ion implantation into GaN is of particular interest as the incorporation of F atoms into AlGaN/GaN heterostructures can be an effective low-cost approach to achieve postepitaxy threshold voltage modulation in AlGaN/GaN high-electron mobility transistors [27].

In order to reveal a particular role of the implanted species on radiation tolerance of GaN we apply combined irradiation schemes where low and high energy implants with different ions were used. We demonstrate that the interplay between defect stabilization by implanted atoms and radiation-stimulated defect annealing determines damage formation in GaN. Depending on the implanted species, these processes can lead either to the amorphization or healing the disorder in the crystal bulk**.**

2. Experimental

About 2.5 μm thick (0001) wurzite epitaxial GaN films grown by MOCVD on sapphire substrate at the Ioffe Institute (St. Petersburg, Russian Federation) were used in this study. Samples were irradiated at room temperature with different ions having low (1.3 keV/amu) and high (3.2 keV/amu) energies (see Table I summarizing the implant parameters used in the present study). The energies of the ions were chosen in such a way to provide a maximum defect generation for the high energy irradiations (as calculated with the SRIM code simulations [28]) as close as possible to the BDP region of the low energy implants. All the implantations were performed at 7° off [0001] direction to minimize channeling effects. In order to compare irradiation effects produced by different ions we use similar doses expressed in displacement per atom (DPA) taken at the maximum of nuclear energy loss. Quoted DPA values were calculated as DPA = $n_v \times \Phi / n_{at}$, where Φ is an ion dose in ions/cm^2, n_v is an average number of vacancies produced per unit of depth by one ion at the depth of maximum of nuclear energy loss, and $n_{at} = 8.85\times10^{22}$ cm^{-3} is the GaN atomic concentration. Values of n_v were calculated using the SRIM code simulations [28] with effective threshold energies for atomic displacements of 25 eV for both Ga and N sublattices. Thus the dose of 1 DPA means that each atom at the depth of R_{pd} has on the average been once shifted from its position. Note that ion fluxes were kept constant at 3.6×10^{-3} DPA/s for all implants to avoid possible dose-rate effects [8].

Implantation-produced disorder was measured by Rutherford backscattering spectrometry in channeling mode (RBS/C) by 0.7 MeV He^{++} ions incident along the [0001] direction and backscattered to 103^o, which improved depth resolution. All RBS/C spectra were analyzed using one of the conventional algorithms [29] to extract the effective number of scattering centers (referred to below as “relative disorder”).

Table 1. Implant parameters used in the present study. Also given are calculated values of the projected ion range (R_p), the maximum of the nuclear energy loss profile (R_{pd}), and the ion fluences corresponding to the dose of 1 DPA.

Ion	Energy keV	Energy keV/amu	R_p nm	R_{pd} nm	1 DPA 10^{14} cm^{-2}	Ion flux 10^{11} cm^{-2}s^{-1}
$^{31}P^+$	40	1.3	31	17	5.61	20.2
$^{31}P^+$	115	3.2	82	52	6.37	22.9
$^{19}F^+$	25	1.3	32	17	10.2	36.7
$^{19}F^+$	61	3.2	76	50	12	43.2
$^{40}Ar^+$	53	1.3	32	17	4.43	15.9
$^{40}Ar^+$	155	3.2	86	54	5.04	18.1
$^{20}Ne^+$	26	1.3	32	16	9.2	33.1

3. Results and discussion

The role of the pre-existing disorder on the damage buildup in the GaN is illustrated in Fig. 1 showing the depth profiles of relative disorder in the samples sequentially implanted with low energy ions (P or F) and high energy ions. It might be seen from Figs. 1(a – c) that both (F and P) low energy pre-implants produce practically the same disorder in the BDP region located around ~40 nm deep as marked in the panel (c). This damage level corresponds to the saturation stage of the disorder accumulation and corroborates well with the previous ion implantation studies of GaN [3, 8, 16]. However, further damage accumulation under additional high energy ion irradiation is dramatically different in the F and P pre-implanted samples. Indeed, high energy irradiation with both F and P ion leads to the rapid damage growth in the low energy BDP region in the F pre-implanted samples (see Fig. 1(a, b)). The disorder growth in this region is so strong that it reaches the random level already after P implantation to 15 DPA (or F implantation to 20 DPA) forming continuous amorphous layer starting from the surface. In contrast, the same high energy P irradiation in the P pre-implanted samples leads to the noticeable decrease of the damage level in the low energy BDP region (Fig. 1(c)). At the same time the damage at the sample surface continues to grow as can be seen from the SAL increase. Note that a peak at the depth of ~120 nm seen in the high dose curves is an artifact attributed to carbon atoms at the sample surface that becomes visible in the RBS spectra after high enough dose collection [30]. It should be emphasized here that the main difference between all these three cases is the ion species used for pre-implantation, while all other irradiation parameters were kept the same (see Table I). Slight dose difference between F and P ion pre-implants (15 and 18 DPA respectively) does not cause any change in the BDP height or position [16, 17]. Thus, the observed difference in the damage buildup clearly demonstrated in Figs. 1(a – c) should be attributed to the effects directly related to the ion species used for pre-implantation.

In order to better understand the damage formation mechanism in GaN and, specifically, the role of the ion species on the damage buildup we performed additional implantations with noble gases (Ar and Ne). So the possible chemical effects on damage formation should be negligible in this case. The results are summarized in Fig. 2 where the relative disorder taken at the low energy BDP maximum depth is plotted as a function of the total DPA value (i.e. low energy pre-implantation DPA + DPA of the high energy irradiation). So, the doses below 15-18 DPA correspond to the low energy ion bombardment, whereas the right part of the figure shows the results of cumulative doses. For example, the point on the curve marked as "F25 + P115" at 25 DPA means that the irradiation was carried out with 25 keV F ions to a dose of 15 DPA and then by 61 keV P ions to a dose of 10 DPA [31]. It can be seen that for all low energy single ion implants (F, P and Ne), the damage follows the same trend with the saturation stage occurring at ~0.4 of the full amorphization level for the DPA values up to ~20. Similar dependence was obtained for low energy Ar ion implantation (not shown). However, the damage accumulation in the co-implanted samples exhibits drastically different behavior depending on the ion species used for the low energy pre-implants. Indeed, there is a rapid damage growth leading to the amorphization for all the samples pre-implanted with F ions, while the co-implantations lead to decrease of the damage in the samples pre-implanted with other ions (P, Ne and Ar).

This intriguing damage behavior in the co-implanted samples can be understood in the framework of the model proposed previously to explain the main damage buildup features in GaN [17]. Indeed, according to this model the damage saturation of BDP occurs due to insufficient concentration of mobile point defects in the vicinity of BDP since its position for high doses is located deeper than the region where the primary defects are generated (see Fig. 1 for clarity). Thus, the high energy implantation acts as an additional source of the mobile point defects in the vicinity of low energy BDP enabling further damage evolution in this region. For instance, a high concentration of vacancy type defects may lead to the efficient defect annihilation in the low energy BDP region where a large concentration of interstitial type defects is expected to be present, as mentioned above. This should lead to radiation-stimulated defect annealing and, therefore, decrease of the damage, as indeed observed in our experiments.

However, chemical effects of the implanted species or ion-defect reactions should play a decisive role on the damage buildup in the F pre-implanted samples. For high enough dose, the concentration of the implanted F atoms could be sufficient for effective stabilization of ion-induced defects forming, for example, F-related complexes. In addition, it is seen from Figs. 1(a,b) and 2 that in the F pre-implanted samples the irradiation with high energy P ions leads to more efficient damage growth, as compared to the high energy F implantation. This enhancement is directly attributed to the nonlinear effects in damage formation which become more pronounced with increasing density of collision cascades (see, for example, [16]).

Thus, it can be concluded that the damage formation in GaN depends on the balance between radiation-stimulated defect annealing and defect stabilization by implanted impurity, such as F atoms. In order to estimate a critical F concentration required for changing the balance and, therefore, for the effective damage growth we prepared the set of samples pre-implanted with combinations of low energy Ne and F ions keeping the total dose value at 15 DPA. The atomic masses of Ne and F are close to each other and, taking into account the irradiation parameters (see Table I), the only difference between these samples was the F/Ne dose ratio. Fig. 3(a) shows the depth profiles of the relative disorder in the Ne+F co-implanted samples and it is seen that the damage profiles practically resemble each other for all the Ne/F combinations used. Thus, identical initial damage distributions were produced with different concentrations of implanted F atoms. After that, additional irradiations were performed with high energy P ions to the dose corresponding to 5 DPA. Fig. 3(b) shows the damage profiles in GaN samples after these combined (Ne+F)+P implantations. It is seen that the final damage after the high energy implantation dramatically depends on the initial F dose. In particular, a strong damage enhancement in the region of low energy BDP is observed for the F dose equal or exceeding 12.5 DPA. The crucial role of the implanted F atoms on the damage behavior in the (Ne+F)+P co-implanted samples is better illustrated by Fig. 4 showing the relative disorder in the low energy BDP maximum as a function of F concentration at R_p in the Ne+F pre-implanted samples. It is seen that radiation-stimulated defect annealing is a dominating process for low F concentrations leading to decrease of the damage after high energy P irradiation. In its turn, strong damage enhancement is observed for high F concentration in excess of ~2×10^{21} cm^{-3} which can be attributed to the F-induced defect stabilization.

The mechanism of damage stabilization by implanted F atoms can be attributed to the formation of defect complexes involving F atoms, as mentioned above. The interaction of F atoms with ion-induced defects and formation of F-related defect complexes in GaN has been studied previously [31-35]. In particular, it was demonstrated that the major species of F-induced defects are vacancy clusters coupled with F atoms [31]. However, the dominant type of F-vacancy complexes involved in to the formation of stable defects remains controversial. For example, it has been found that F diffusion in GaN occurs via Ga vacancy (V_{Ga}) assisted mechanism [33]. Furthermore, single V_{Ga} has been identified as the main vacancy-type defect in F implanted GaN samples as detected by positron-annihilation spectroscopy [3130]. In its turn, Takahashi *et al.* [35] demonstrated that F atoms tend to form complexes with nitrogen vacancies (V_N) and suggested that F-V_N complexes may act as a major donor compensation defect in Mg implanted GaN.

Finally, a certain importance of a/c interface for the damage saturation/growth in BDP region of GaN should be emphasized. Indeed, as it was demonstrated previously, efficient trapping and annihilation of the generated point defects at the a/c interface can limit the defect concentration in the vicinity of BDP [17, 18]. Therefore, the processes of damage accumulation in the crystal bulk depend to the large extent on the proximity of the a/c interface to the BDP region. This, in particular, implies that the BDP growth increases with increasing energy of the implanted element if the concentration of implanted atoms is high enough to trigger efficient defect stabilization in this region. Such behavior was indeed observed for room temperature implantations with 61 keV F ions (present study, not shown) and 40 keV C implants in GaN [8].

4. Conclusions

In conclusion, we have studied structural disorder in GaN under combined ion irradiations. The implant parameters were chosen in such a way to reveal basic mechanisms of defect formation in the crystal bulk. We demonstrated that disorder accumulation in the GaN bulk depends on the interplay between radiation-stimulated defect annealing and defect stabilization by implanted atoms. The balance between these two processes depends on the implanted species and, specifically, for F ions strong damage enhancement was observed in the region where F concentration is maximal. The critical concentration of implanted F atoms required for efficient defect stabilization was estimated to be of $\sim 2\times10^{21}$ cm^{-3}.

5. Acknowledgements

Authors are grateful to Dr. W. Lundin (Ioffe Institute, St. Petersburg, Russia) for kind supplying of GaN samples used in this study. Work at St.-Petersburg is partially funded by the Ministry of Science and Higher Education of the Russian Federation under the strategic academic leadership program 'Priority 2030' (Agreement 075-15-2021-1333 dated 30.09.2021). AA acknowledges Research Centre for Sustainable Solar Cell Technology (FME SuSolTech, project number 257639) co-sponsored by the Research Council of Norway and industry partners.

DATA AVAILABILITY

The data that support the findings of this study are available from the corresponding author upon reasonable request.

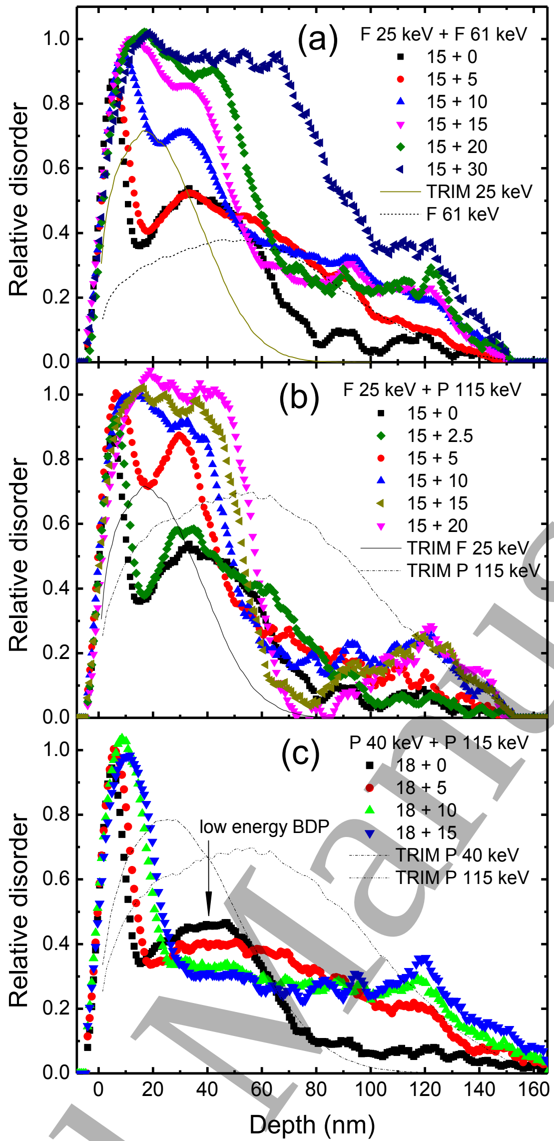

Fig. 1 Depth profiles of relative disorder produced by 61 keV F^+ ions in GaN samples pre-implanted with 25 keV F^+ ions (a), as well as by 115 keV P^+ ions in samples pre-implanted with 25 keV F^+ ions (b) and 40 keV P^+ ions (c). The doses in DPA are indicated in the legends where the first number is related to the pre-implantation and the second one corresponds to the high energy implant. The SRIM predicted profiles of total vacancies after implantation with 25 and 61 keV F ions (a), 25 keV F and 115 keV P ions (b), and 40 keV and 115 keV P ions (c) are shown in the corresponding panels in arbitrary units.

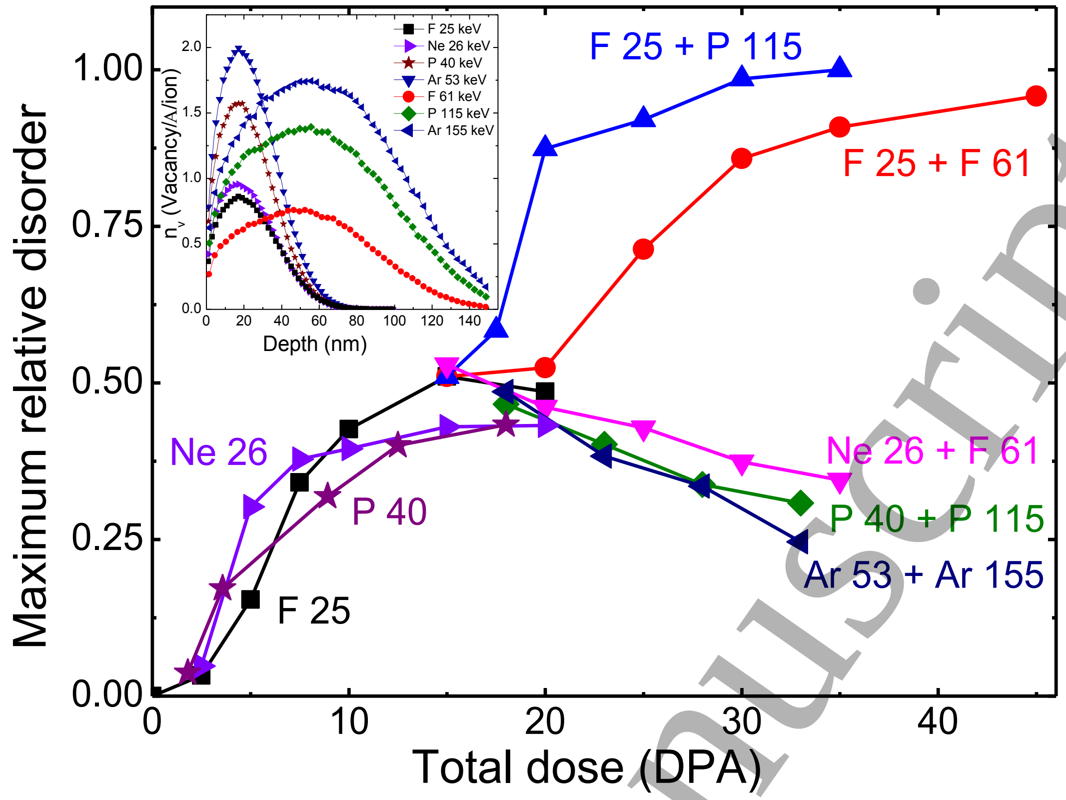

Fig. 2 Maximum relative disorder, taken at the depth of the low energy BDP maximum, as a function of the total dose of ions of both energies. The ions, their energies as well as ion combinations used in the present study are indicated in the legend. The inset shows TRIM simulated vacancy generation profiles for all cases.

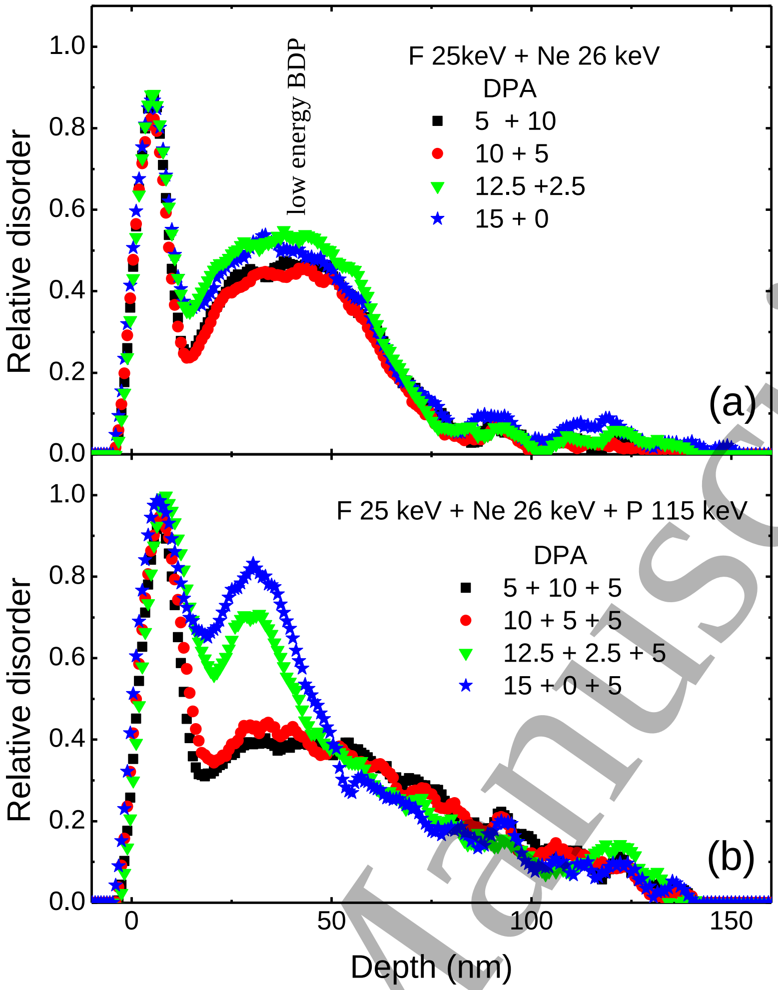

Fig. 3 Depth profiles of the relative disorder in GaN samples sequentially irradiated with 25 keV F and 26 keV Ne ions to the total dose of 15 DPA, and (b) additionally implanted with high energy 115 keV P ions to 5 DPA. The DPA values of F, Ne and P ion irradiations are indicated in the legends.

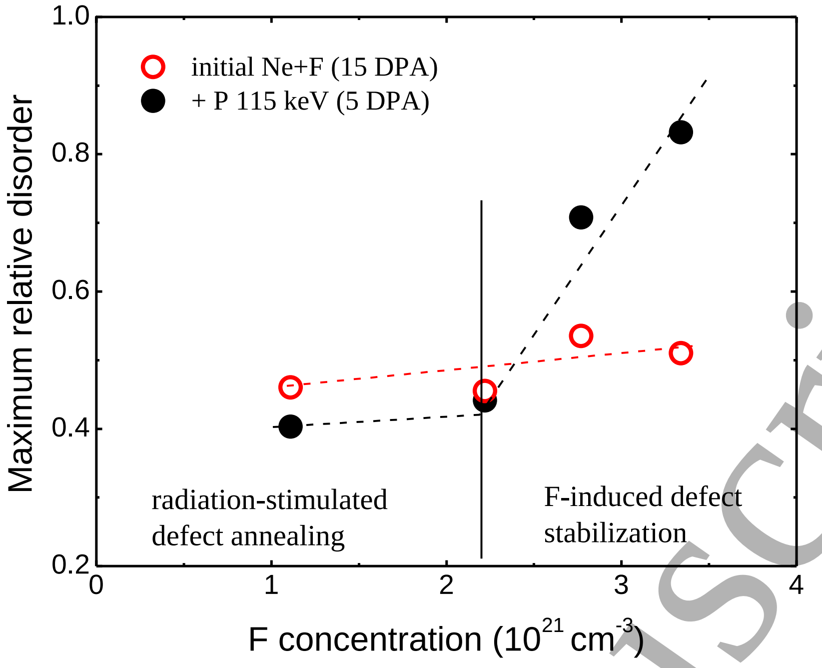

Fig. 4 Relative disorder in the low energy BDP maximum as a function of the F concentration in the co-implanted (Ne+F)+P samples. Open symbols correspond to the initial damage level in the samples pre-implanted with (Ne+F) ions to the total dose corresponding to 15 DPA. Closed symbols indicate the damage after the final high energy irradiation performed by 115 keV P^+ ions to a dose of 5 DPA. The dashed lines are to guide the eye.

References

1. S. J. Pearton, F. Ren, E. Patrick, M. E. Law, and A. Y. Polyakov, "Review—Ionizing Radiation Damage Effects on GaN Devices", ECS Journal of Solid State Science and Technology **5**, Q35 (2016).

2. M. T. Robinson, "Basic physics of radiation damage production", J. Nucl. Materials **216**, 1 (1994).

3. E. Wendler, "Mechanisms of damage formation in semiconductors", Nucl. Instrum. and Meth. Phys. Res. B **267**, 2680 (2009).

4. U. K. Mishra, L. Shen, T. E. Kazior, and Y.-F. Wu, "GaN-Based RF Power Devices and Amplifiers", Proc. IEEE **96**, 287 (2008).

5. K. Ahi, "Review of GaN-based devices for terahertz operation", Optical Engineering **56,** 090901 (2017).

6. K. J. Chen, O. Häberlen, A. Lidow, C. L. Tsai, T. Ueda, Y. Uemoto, and Y. Wu, "GaN-on-Si Power Technology: Devices and Applications", IEEE Trans. Electron Devices **64**, 779 (2017).

7. C. Liu, B. Mensching, M. Zeitler, K. Volz, and B. Rauschenbach, "Ion implantation in GaN at liquid-nitrogen temperature: Structural characteristics and amorphization", Phys. Rev. B **57**, 2530 (1998).

8. S. O. Kucheyev, J. S. Williams, and S. J. Pearton, "Ion implantation into GaN", Mater. Sci. Eng. R **33**, 51 (2001).

9. C. Ronning, E. P. Carlson, and R. F. Davis, "Ion implantation into gallium nitride", Physics Reports **351**, 349 (2001).

10. Y. Zhang, M. Ishimaru, J. Jagielski, W. Zhang, Z. Zhu, L. V. Saraf, W. Jiang, L. Thome, and W. J. Weber, "Damage and microstructure evolution in GaN under Au ion irradiation", J. Phys. D: Appl. Phys. 43, 085303 (2010).

11. P. Ruterana, B. Lacroix, and K. Lorenz, "A mechanism for damage formation in GaN during rare earth ion implantation at medium range energy and room temperature", J. Appl. Phys. **109**, 013506 (2011).

12. M. Ishimaru, Y. Zhang, and W. J. Weber, "Ion-beam-induced chemical disorder in GaN", J. Appl. Phys. **106**, 053513 (2009).

13. K. Lorenz, E. Wendler, A. Redondo-Cubero, N. Catarino, M.-P. Chauvat, S. Schwaiger, F. Scholz, E. Alves, and P. Ruterana, "Implantation damage formation in a-, c- and m-plane GaN", Acta Materialia **123**, 177 (2017).

14. J. Wiang, Y. Zhang, W. J. Weber, J. Lian, R. C. Ewing, "Direct evidence of N aggregation and diffusion in Au^+ irradiated GaN", Appl. Phys. Lett. **89**, 021903 (2006).
15. K. Lorenz, N. P. Barradas, E. Alves, I. S. Roqan, E. Nogales, R. W. Martin, K. P. O'Donnell, F. Gloux, and P. Ruterana, "Structural and optical characterization of Eu-implanted GaN", J. Phys. D: Appl. Phys. **42**, 165103 (2009).
16. S. O. Kucheyev, A. Yu. Azarov, A. I. Titov, P. A. Karaseov, and T. M. Kuchumova, "Energy spike effects in ion-bombarded GaN", J. Phys. D: Appl. Phys. **42**, 085309 (2009).
17. A. I. Titov, P. A. Karaseov, A. Yu. Kataev, A. Yu. Azarov, and S. O. Kucheyev, "Model for radiation damage buildup in GaN", Nucl. Instrum. Meth. Phys. Res. B **277**, 80 (2012).
18. A. Yu. Azarov, A. I. Titov, and S. O. Kucheyev, "Effect of pre-existing disorder on surface amorphization in GaN", J. Appl. Phys. **108**, 033505 (2010).
19. A. Azarov, P. Rauwel, A. Hallén, E. Monakhov, and B. G. Svensson, "Extended defects in ZnO: Efficient sinks for point defects", Appl. Phys. Lett. **110**, 022103 (2017).
20. A. Turos, "On the mechanism of damage buildup in gallium nitride", Radiation Effects & Defects in Solids **168**, 431 (2013).
21. M. C. Sequeira, J.-G. Mattei, H. Vazquez, F. Djurabekova, K. Nordlund, I. Monnet, P. Mota-Santiago, P. Kluth, C. Grygiel, S. Zhang, E. Alves, and K. Lorenz, "Unravelling the secrets of the resistance of GaN to strongly ionising radiation", Comm. Phys. **4**, 51 (2021).
22. A. I. Titov, K. V. Karabeshkin, P. A. Karaseov, and A. I. Struchkov, "The formation of radiation damage in GaN during successive bombardment by light ions of various energies", Vacuum **173**, 109149 (2020).
23. S. O. Kucheyev, J. E. Bradby, C. P. Li, S. Ruffell, T. van Buuren, and T. E. Felter, "Effects of carbon on ion-implantation-induced disorder in GaN", Appl. Phys. Lett. **91**, 261905 (2007).
24. X. F. Li, Z. Q. Chen, C. Liu, H. J. Zhang, and A. Kawasuso, "Enhanced damage buildup in C^+-implanted GaN film studied by a monoenergetic positron beam", J. Appl. Phys. **117**, 085706 (2015).
25. A. I. Titov, K. V. Karabeshkin, P. A. Karaseov, and A. I. Struchkov, "Do Chemical Effects Affect the Accumulation of Structural Damage during the Implantation of Fluorine Ions into GaN?", Semiconductors **53**, 1415 (2019).
26. A. I. Struchkov, K. V. Karabeshkin, A. V. Arkhipov, V. A. Filatov, P. A. Karaseov, A. Azarov, A. I. Titov, "Impact of Chemical Effects on Topography and Thickness of Modified GaN Surface Layers Bombarded by F and Ne Ions", in In: Velichko E., Vinnichenko M., Kapralova V., Koucheryavy Y. (eds)

International Youth Conference on Electronics, Telecommunications and Information Technologies. Springer Proceedings in Physics **255**, p. 151. Springer, Cham (2020)

27. Y. Cai, Y. Zhou, K. M. Lau, and K. J. Chen, "Control of Threshold Voltage of AlGaN/GaN HEMTs by Fluoride-Based Plasma Treatment: From Depletion Mode to Enhancement Mode", IEEE Trans. on Electron Devices **53**, 2207 (2006).
28. J. F. Ziegler, M. D. Ziegler, J. P. Biersack, "SRIM – The stopping and range of ions in matter (2010)", Nucl. Instrum. Methods Phys. Res. B **268**, 1818 (2010); SRIM-2013 software package http://www.srim.org.
29. K. Schmid, "Some new aspects for the evaluation of disorder profiles in silicon by backscattering", Rad. Effects **17**, 201 (1973).
30. Scattering of probing He on carbon atoms situated on the target surface gives rise to the peak at the RBS channels that correspond to ~120 nm. Indeed, this peak becomes visible when certain carbon layer thickness is formed, i.e. after high enough dose collection. Certainly, some carbon recoils could be implanted into GaN during high dose irradiation. However, their amount would be negligible, and more important, penetration depth of these atoms would be very small compare to the depth at which the discussed effects are observed.
31. Adding of DPAs for low and high energy implantation gives cumulative DPA value that refers to the amount of displacements at the depths corresponding to the low energy ion R_{pd} position.
32. M. J. Wang, L. Yuan, C. C. Cheng, C. D. Beling, and K. J. Chen, "Defect formation and annealing behaviors of fluorine-implanted GaN layers revealed by positron annihilation spectroscopy", Appl. Phys. Lett. **94**, 061910 (2009).
33. M. J. Wang, L. Yuan, K. J. Chen, F. J. Xu, and B. Shen, "Diffusion mechanism and the thermal stability of fluorine ions in GaN after ion implantation", J. Appl. Phys. **105**, 083519 (2009).
34. A. Uedono, N. Yoshihara, Y. Zhang, M. Sun, D. Piedra, T. Fujishima, S. Ishibashi, M. Sumiya, O. Laboutin, W. Johnson, and T. Palacios, "Vacancy clusters introduced by CF_4-based plasma treatment in GaN probed with a monoenergetic positron beam", Appl. Phys. Express **7**, 121001 (2014),
35. M. Takahashi, A. Tanaka, Y. Ando, H. Watanabe, M. Deki, M. Kushimoto, S. Nitta, Y. Honda, K. Shima, K. Kojima, S. F. Chichibu, K. J. Chen, and H. Amano, "Suppression of Green Luminescence of Mg-Ion-Implanted GaN by Subsequent Implantation of Fluorine Ions at High Temperature", Phys. Status Solidi B **257**, 1900554 (2020).